Influence of NOM Concentration on Parameter Sensitivity of a Mechanistic Ozone Decomposition Model

W. T. M. Audenaert*,**, M. Vandevelde*, S. W. H. Van Hulle*,** and I. Nopens**

* ENBICHEM, Department of Industrial Engineering and Technology, University College West Flanders, Graaf Karel de Goedelaan 5, 8500 Kortrijk
(E-mail: *wim.audenaert@howest.be; mathieu.vandevelde@howest.be; stijn.van.hulle@howest.be)*
** BIOMATH, Department of Applied Mathematics, Biometrics and Process Control, Ghent University, Coupure Links 653, 9000 Gent
(E-mail: *ingmar.nopens@ugent.be*)

Abstract
Aqueous ozone decomposition proceeds through a complex chain mechanism of radical reactions. When natural organic matter (NOM) is present, the system becomes much more complex and often (semi-)empirical modelling approaches are used to describe ozonation of water and wastewater systems. Mechanistic models, however, can be of great value to gain knowledge in the chemical pathways of ozonation and advanced oxidation processes in view of engineering applications. However, the numerous model parameters and model complexity often restrict their applicability. Model simplification is then an option to cure these drawbacks. In this study, sensitivity analyses (SAs) were used to determine the most important elementary reactions from the complex kinetic model. Additionally, SAs were used to understand the reaction mechanism. It was demonstrated that only seven of the twenty-eight first and second order rate constants showed to impact ozone and $HO^{\bullet}$ concentrations. Processes involving $HO^{\bullet}$ scavenging by inorganic carbon were of minor importance. Mass-transfer related parameters k_La and $[O_3^*]$ were of major importance in all cases. Hence, it is of extreme importance that these parameters are determined with high accuracy. It was shown that the aqueous ozone concentration is extremely sensitive to parameters involving NOM at very low scavenger concentrations implying that impurities should always be considered in models, even in ultrapure water systems. Uncertainty analysis showed that especially the $HO^{\bullet}$ concentration is susceptible to variations in influent composition. The uncertainty regarding this species significantly reduced with increasing levels of scavengers and especially NOM. It was demonstrated that simplification of the elementary radical scheme should be considered. On the other hand, a model extension with regard to reactions involving NOM should be performed in order to improve the applicability of future wastewater ozonation models.

Keywords
advanced oxidation processes, model calibration, NOM, sensitivity analysis, UV absorption, UV/H_2O_2

1. INTRODUCTION

The use of ozone in water treatment is an established technique for several decades. Ozone is known as a strong disinfectant which produces less disinfection by-products than chlorine when appropriate doses are applied. Additionally, due to its oxidative power, ozone is able to selectively attack specific moieties of micropollutants to produce harmless metabolites (Buffle et al., 2006b). These properties gave rise to numerous full-scale applications in drinking water treatment worldwide. Moreover, the application of ozone in (biological) wastewater treatment is recently gaining interest, especially as an oxidative tertiary treatment step (Zimmermann et al., 2011).

Nowadays, a vast amount of research still focuses on mechanisms involving water and wastewater ozonation and (advanced) oxidation in general, and related to this, the role of dissolved organic matter in these processes (Buffle et al., 2006a; Buffle et al., 2006b; Elovitz and von Gunten, 1999; Van Geluwe et al., 2011; Westerhoff et al., 1999; Westerhoff et al., 2007). The complexity of the aqueous organic matrix and oxidant induced molecular conversions severely impede efforts to describe the oxidation processes in a mechanistic way. In most natural waters and wastewaters, the organic matrix can be classified as natural organic matter (NOM). NOM is a complex heterogeneous mixture of dissolved organic material that can be divided into several classes of which in some cases the exact composition still remains unknown (Van Geluwe et al., 2011). The goal of the earlier mentioned studies is mainly to gain fundamental knowledge on the oxidation kinetics in order to provide detailed models that can have various applications. Adequate mathematical models can be used to engineer, optimize and control the treatment process. A key issue in all model applications is the assessment of oxidant exposures. This is an important process factor that determines disinfection and oxidation efficacy. Prediction of micropollutant oxidation can be of great value as laboratory analysis is laborious and resource intensive and no online measurement methods exist (Neumann et al., 2009).

Aqueous ozone decomposition proceeds through a complex chain mechanism of radical reactions. A general accepted reaction sequence for ozone decomposition in ultrapure water at acidic to neutral pH is the Staehelin-Bühler-Hoigné (SBH) model (Buhler et al., 1984; Staehelin et al., 1984). In natural water and wastewater where NOM is present, the system becomes much more complex and often empirical approaches are used to model the ozonation process. Often, this is due to a lack of detailed information on reaction pathways of NOM and the uncertainty associated with the use of detailed elementary mechanisms in real systems (these reaction schemes were initially defined at well known and controlled conditions in ultrapure water). Empirical models can be of value for some cases but lack flexibility to be applied over a wide range of conditions (Westerhoff et al., 1997). Additionally, extensive experimental data collection is needed to construct these models. There are, however, some important semi-empirical relations that have already proven to be very useful to model natural water ozonation. The use of first (or sometimes higher) reaction orders to model ozone decay in the presence of slow reacting organic matter compounds is well known (Westerhoff et al., 1999). This approach was used in numerous studies to calculate the aqueous ozone concentration as function of time and hence, the disinfection or oxidation progress. As already indicated, aqueous ozone decomposition gives rise to radicals. The hydroxyl radical ($HO^{\bullet}$) is proven to significantly enhance micropollutant oxidation during conventional ozonation (Buffle et al., 2006b; Zimmermann et al., 2011). This implies that both ozone and $HO^{\bullet}$ exposures should be calculated in order to accurately model the oxidation process. A semi-empirical approach to determine hydroxyl radical exposure which is proven to be very useful in water treatment is the R_{ct} concept developed by Elovitz and von Gunten (1999). This concept is based on the assumption that the ratio of $HO^{\bullet}$ and ozone exposure remains constant throughout the ozonation process (Elovitz and von Gunten, 1999). Consequently, the $HO^{\bullet}$ concentration (and exposure) can be simply calculated based on the measured ozone concentration and R_{ct} value (the latter is water-dependent and known from a preliminary

experiment) (Elovitz and von Gunten, 1999). The R_{ct} concept allows for the use of literature-established second order rate constants for ozone and $HO^{\bullet}$ based oxidation to predict micropollutant concentrations. Additionally, the relative importance of direct and indirect oxidation in the process can be studied (Buffle et al., 2006b; Elovitz and von Gunten, 1999; Zimmermann et al., 2011). It was shown, however, that the use of the R_{ct} concept and a single first order ozone decay constant are less suited to describe wastewater ozonation because these parameters are likely to change as function of oxidation time (Buffle et al., 2006a; Buffle et al., 2006b). Furthermore, natural water and wastewater ozonation may differ mechanistically as DOM moieties and corresponding metabolites were proven to exhibit significantly different absorbance spectra (Westerhoff et al., 2007). Hence, more complex mechanistic models are required.

The well-established SBH sequence can be a good starting point for the construction of wastewater ozonation models. Many earlier applications of this model, however, showed poor agreement between experimental determined and predicted ozone concentration profiles (Bezbarua and Reckhow, 2004; Elovitz and von Gunten, 1999; Fabian, 2006; Lovato et al., 2009). Often, the literature values of the elementary rate constants were questioned and proposed to be the main reason for the disagreement. Hence, often one or more elementary rate constants of the extensive mechanisms are re-evaluated in order to obtain better fits (Bezbarua and Reckhow, 2004; Fabian, 2006; Lovato et al., 2009). This recalibration, however, does not rely on chemical or kinetic knowledge and thus implies that the originally well-defined models shift to the empirical side. In these cases, a modification of elementary kinetic constants compensates for important mechanistic knowledge that is missing in the model structure. In order to balance the model complexity, a simplification of the radical scheme (SBH model) on the one hand and an extension of the NOM reaction scheme on the other hand is recommended.

Prior to simplification or modification of a complex kinetic model, it is useful to analytically determine the most important elementary reactions. A sensitivity analysis (SA) is suitable for this purpose (Saltelli et al., 2005). This mathematical tool allows to quantify the sensitivity of one or more variables towards certain parameters of interest. Despite the benefits, literature reported applications of SAs on kinetic oxidation models are scarce. Neumann et al. (2009) conducted a global SA on a drinking water ozonation model (Neumann et al., 2009). To model ozone decay, a first order rate law was used and the $HO^{\bullet}$ exposure was calculated by means of the R_{ct} concept. It was shown that R_{ct} is an extremely influential parameter with respect to the concentration of pollutants that are susceptible to $HO^{\bullet}$ attack (Neumann et al., 2009). This again may indicate that the R_{ct} approach is not suitable for wastewater ozonation because the value of R_{ct} becomes even more uncertain. The first order ozone decay constant seemed to be less important. Audenaert et al. (2010) performed a local SA on a simple model that was used to predict residual ozone, bromate formation, NOM oxidation and disinfection. In this study, parameters related to NOM were found to be of major importance. The first order ozone decay constant was again regarded as less important. Audenaert et al. (2011) used an extensive UV/hydrogen peroxide advanced oxidation model to describe a full-scale reactor. The model consisted of a set of elementary radical reactions, comparable to the SBH

model. A local sensitivity analysis revealed that with respect to the $HO^{\bullet}$ concentration, scavenging by hydrogen peroxide and bicarbonate were most important. The kinetic constant describing $HO^{\bullet}$ scavenging by NOM just slightly affected the $HO^{\bullet}$ concentration because of the existence of two counteracting processes. An increase of this parameter enhanced the $HO^{\bullet}$ scavenging rate on the one hand, but gave rise to a better UV transmission on the other hand, leading to an increased $HO^{\bullet}$ production rate. Nine second order rate constants were found to exert no influence to the variables at all and micropollutant concentrations were found to be very influential to many of the parameters (Audenaert et al., 2011). Lovato et al. (2009) used the SBH model as a starting point for their study (Lovato et al., 2009). A poor fit between the experimental and modeled ozone concentration was the rationale for modifying the standard kinetic scheme. The model adaptation, however, was not based on a sensitivity analysis. The impact of the model parameters on the ozone concentration was determined by changing each parameter separately to a higher and lower value on an arbitrary basis. For every parameter change, a new simulation was run and the overall ozone decay rate was studied. By making one rate constant pH dependent, a good fit could be obtained (Lovato et al., 2009). In another study, these authors used a modified version of the SBH model (Lovato et al., 2011). The mechanism was reduced from 31 to 23 reaction steps based on a sensitivity analysis (Lovato et al., 2011). It was, however, not totally clear what these authors meant with sensitivity analysis, how it was performed and on which basis eight elementary reactions were removed. Fabian et al. (2006) questioned the validity of the original SBH model and highlighted the uncertainty associated with literature reported values of the kinetic parameters. The model was recalibrated by means of an optimization algorithm (Fabian, 2006). Additionally, four elementary reactions were discarded based on a sensitivity analysis. Again, it was not very clear how this sensitivity analysis was performed and how it was decided to simplify the model.

In contrast to some previous studies, the SA in this study was based on a structured approach. The SBH model as described by Bezbarua and Reckhow (2006) was used and the reaction scheme was extended with a single equation to describe $HO^{\bullet}$ scavenging by NOM. Hence, the main focus here was to study the SBH scheme, rather than to construct a complicated model including mass balances of different NOM moieties. Local and global SAs were conducted over a wide range of NOM and bicarbonate concentrations. The goals of this study were to: (i) determine the most important elementary reactions of the sequence, (ii) get insight into the reaction mechanism by distinguishing different phases (switches in local sensitivity functions) occurring during ozonation in the presence of NOM at different concentrations and (iii) compare the results and corresponding conclusions of the local and global approach to perform SAs.

2. METHODS

2.1. Model conceptualization

A reactor continuously fed with gaseous ozone was simulated using the SBH model as described by Bezbarua and Reckhow (2006). The model was extended with a simple second order equation describing the reaction between hydroxyl radicals and NOM, expressed as dissolved organic matter (DOM). The model assumed that only hydroxyl radicals (not ozone) decomposed DOM with a molar ratio of 1:1 and a second order rate constant of 2×10^8 M^{-1} s^{-1} (Westerhoff et al., 1997). Hence, DOM in this study merely acted as inhibitor serving as a sink for $HO^{\bullet}$. Additionally, a gas-liquid mass transfer equation was added to account for the gaseous ozone inflow. The reaction system is schematically presented in Table 1. In this Gujer matrix (Henze et al., 2000), the different elementary processes are indicated in the left column. The components shown at the top of the table represent the derived state variables (mole L^{-1}) which have to be calculated with numerical integration. Reaction products such as oxygen or water that do not have a mass balance are not included in the table. The right column contains the reaction rates of each individual process. The square brackets indicate the concentration of the compound enclosed in the brackets, expressed in mole L^{-1}. Finally, the central matrix elements are stoichiometric factors used in the mass balances. Mass balances can be easily built up by multiplying each matrix element of one column (one variable) by the reaction rate at the same row of the element. A summation of these products yields the conversion terms of the mass balance (Henze et al., 2000). After addition of the transport terms, the complete mass balances can be recovered. A detailed description of composing the mass balances is given in the Appendix. This Gujer matrix notation is an elegant way to summarize a set of ordinary differential equations and gives a clear overview of all elementary reactions occurring during the process. More information about the parameters and their values can be found in Table 2.

Table 1: Gujer matrix presentation of the reaction system

Process	**Components**														**Reaction rate**
	O_3	**HO_2^-**	**HO_2•**	**O_2^-•**	**O_3^-•**	**HO_3•**	**OH•**	**H_2O_2**	**CO_3^-•**	**DOM**	**CO_3^{2-}**	**CO_2**	**HCO_3^-**	**HCO_3•**	
Chain initiation															
$O_3 + OH^- \rightarrow HO_2^- + O_2$	-1	1													$k_1 \times [O_3] \times [OH^-]$
$O_3 + HO_2^- \rightarrow HO_2^\bullet + O_3^{-\bullet}$	-1	-1	1		1										$k_2 \times [O_3] \times [HO_2^-]$
Chain propagation															
$HO_2^\bullet \rightarrow O_2^{-\bullet} + H^+$			-1	1											$k_3 \times [HO_2^\bullet]$
$O_2^{-\bullet} + H^+ \rightarrow HO_2^\bullet$			1	-1											$k_4 \times [O_2^{-\bullet}] \times [H^+]$
$O_3 + O_2^{-\bullet} \rightarrow O_3^{-\bullet} + O_2$	-1			-1	1										$k_5 \times [O_3] \times [O_2^{-\bullet}]$
$O_3^{-\bullet} + H^+ \rightarrow HO_3^\bullet$					-1	1									$k_6 \times [O_3^{-\bullet}] \times [H^+]$
$HO_3^\bullet \rightarrow O_3^{-\bullet} + H^+$					1	-1									$k_7 \times [HO_3^\bullet]$
$HO_3^\bullet \rightarrow HO^\bullet + O_2$						-1	1								$K_8 \times [HO_3^\bullet]$
$O_3 + HO^\bullet \rightarrow HO_2^\bullet + O_2$	-1		1				-1								$k_9 \times [O_3] \times [HO^\bullet]$
$HO^\bullet + H_2O_2 \rightarrow HO_2^\bullet + H_2O$			1				-1	-1							$k_{10} \times [HO^\bullet] \times [H_2O_2]$
$H_2O_2 \rightarrow HO_2^- + H^+$		1						-1							$k_{11} \times [H_2O_2]$
$HO_2^- + H^+ \rightarrow H_2O_2$		-1						1							$k_{12} \times [HO_2^-] \times [H^+]$
Carbonate reactions															
$CO_2 + H_2O \rightarrow HCO_3^- + H^+$												-1	1		$k_{13} \times [CO_2]$
$HCO_3^- + H^+ \rightarrow CO_2 + H_2O$												1	-1		$k_{14} \times [HCO_3^-] \times [H^+]$
$HCO_3^- \rightarrow CO_3^{2-} + H^+$											1		-1		$k_{15} \times [HCO_3^-]$
$CO_3^{2-} + H^+ \rightarrow HCO_3^-$											-1		1		$k_{16} \times [CO_3^{2-}] \times [H^+]$
$HO^\bullet + HCO_3^- \rightarrow HCO_3^\bullet + OH^-$							-1						-1	1	$k_{17} \times [HO^\bullet] \times [HCO_3^-]$
$HO^\bullet + CO_3^{2-} \rightarrow CO_3^{-\bullet} + OH^-$							-1		1		-1				$k_{18} \times [\ HO^\bullet] \times [\ CO_3^{2-}]$
$HCO_3^\bullet \rightarrow CO_3^{-\bullet} + H^+$									1					-1	$k_{19} \times [HCO_3^\bullet]$
$CO_3^{-\bullet} + H^+ \rightarrow HCO_3^\bullet$									-1					1	$k_{20} \times [CO_3^{-\bullet}] \times [H^+]$
$CO_3^{-\bullet} + CO_3^{-\bullet} \rightarrow 2CO_3^{2-}$									-2		2				$k_{21} \times [CO_3^{-\bullet}]^2$
$CO_3^{-\bullet} + O_2^{-\bullet} \rightarrow CO_3^{2-} + O_2$				-1					-1		1				$k_{22} \times [CO_3^{-\bullet}] \times [O_2^{-\bullet}]$
$CO_3^{-\bullet} + HO_2^- \rightarrow CO_3^{2-} + O_3$	1				-1				-1		1				$k_{23} \times [CO_3^{-\bullet}] \times [HO_2^-]$
$CO_3^{-\bullet} + O_3^{-\bullet} \rightarrow CO_3^{2-} + HO_2^\bullet$		-1	1						-1		1				$k_{24} \times [CO_3^{-\bullet}] \times [O_3^{-\bullet}]$
$CO_3^{-\bullet} + H_2O_2 \rightarrow HCO_3^- + HO_2^\bullet$			1					-1	-1				1		$k_{25} \times [CO_3^{-\bullet}] \times [H_2O_2]$
$CO_3^{-\bullet} + HO^\bullet \rightarrow CO_2 + HO_2^-$		1					-1		-1			1			$k_{26} \times [CO_3^{-\bullet}] \times [HO^\bullet]$
DOM reaction															
$CO_3^{-\bullet} + DOM \rightarrow CO_3^{2-} + products$									-1	-1	1				$k_{27} \times [CO_3^{-\bullet}] \times [DOM]$
$HO^\bullet + DOM \rightarrow products$							-1			-1					$k_{28} \times [HO^\bullet] \times [DOM]$
Mass transfer	1														$k_La \times ([O_3^*] - [O_3])$

Table 2: Parameters of the kinetic model and their values

Parameters	Value		Source
Rate constants			
k_1	70	$M^{-1}s^{-1}$	(Bezbarua and Reckhow, 2004)
k_2	2.8×10^6	$M^{-1}s^{-1}$	
k_3	3.2×10^5	s^{-1}	
k_4	2×10^{10}	$M^{-1}s^{-1}$	
k_5	1.6×10^9	$M^{-1}s^{-1}$	
k_6	5.2×10^{10}	$M^{-1}s^{-1}$	
k_7	3.3×10^2	s^{-1}	
k_8	1.1×10^5	s^{-1}	
k_9	2×10^9	$M^{-1}s^{-1}$	
k_{10}	2.7×10^7	$M^{-1}s^{-1}$	
k_{11}	4.5×10^2	s^{-1}	
k_{12}	2×10^{10}	$M^{-1}s^{-1}$	
k_{13}	2.1×10^4	s^{-1}	(Westerhoff et al., 1997)
k_{14}	5×10^{10}	$M^{-1}s^{-1}$	
k_{15}	2.8	s^{-1}	
k_{16}	5×10^{10}	$M^{-1}s^{-1}$	
k_{17}	8×10^6	$M^{-1}s^{-1}$	
k_{18}	3.7×10^8	$M^{-1}s^{-1}$	
k_{19}	13	s^{-1}	
k_{20}	5×10^{10}	$M^{-1}s^{-1}$	
k_{21}	2×10^7	$M^{-1}s^{-1}$	
k_{22}	4×10^8	$M^{-1}s^{-1}$	
k_{23}	5.6×10^7	$M^{-1}s^{-1}$	
k_{24}	6×10^7	$M^{-1}s^{-1}$	
k_{25}	8×10^5	$M^{-1}s^{-1}$	
k_{26}	3×10^9	$M^{-1}s^{-1}$	
k_{27}	1×10^7	$M^{-1}s^{-1}$	
k_{28}	2×10^8	$M^{-1}s^{-1}$	
Reactor parameters			
k_La	1.7×10^{-3}	s^{-1}	Experimental work
$[O_3^*]$	6.25×10^{-5}	M	Experimental work
V	1	L	This study
Q	4	$L\ h^{-1}$	This study

2.2. Simulations

The system, consisting of 30 parameters and 14 ordinary differential equations (ODEs), was implemented in the generic modeling and simulation platform WEST® (Vanhooren et al., 2003) distributed by DHI (mikebydhi.com). Simulations were run in its associated kernel Tornado® which allows to rapidly numerically simulate the stiff system of differential

equations. The stiff solver CVODE (Hindmarsh and Petzold, 1995) was used for all numerical integrations with an absolute and relative tolerance of 1 x 10^{-20} and 1 x 10^{-5}, respectively.
Two different single-reactor configurations were simulated: (i) a completely stirred semi-batch reactor (continuous gaseous ozone inflow, no water flow) and (ii) a completely stirred tank reactor fed in flow-through mode (continuous gaseous ozone inflow, continuous influent and effluent water flow). Initial DOM concentrations were varied between 0 and 12 mg L^{-1} (0-1 mM) in the different simulations, thus ranging from ultra-pure water concentrations to natural water levels. Total carbonate concentrations (C_T) ranged between 0 and 3.6 mM. For the continuous flow reactor, influent concentrations were set equal to the initial conditions and a fixed flow rate (Q) of 4 L h^{-1} was applied. The initial conditions used for each simulation are presented in Table 3. Initial values for the radical species were derived from Bezbarua and Reckhow (2004). Each simulation in this study was based on the same scenario: at time t=0, the gaseous ozone flow was switched on, after which the aqueous ozone concentration started to build up ($[O_3]_{t=0}$=0). Every simulation was run for at least 5000 seconds. The pH was fixed at 7.5 by implementing fixed concentrations for H^+ and OH^- ions.

Table 3: Initial conditions used for each simulation

Component	Concentration (M)	Component	Concentration (M)
O_3	0	$CO_3^{\bullet-}$	0
HO_2^-	1 x 10^{-12}	DOM	0-1 x 10^{-3}
$HO_2^\bullet$	5 x 10^{-14}	H^+	3,16 x 10^{-8}
$O_2^{\bullet-}$	5 x 10^{-14}	OH^-	3,16 x 10^{-7}
$O_3^{\bullet-}$	4 x 10^{-12}	CO_3^{2-}	0
$HO_3^\bullet$	1 x 10^{-13}	CO_2	0
$OH^\bullet$	5 x 10^{-14}	HCO_3^-	0.4-3.6 x 10^{-3}
H_2O_2	5 x 10^{-9}	$HCO_3^\bullet$	0

2.3. Local sensitivity analysis

Local sensitivity analyses were used to investigate and quantify the influence each model parameter exerts on certain variables of interest. Additionally, local SAs were performed to get insight into the reaction mechanism by distinguishing different phases (switches in local sensitivity functions) occurring during ozonation in the presence of NOM at different concentrations. To allow comparison between sensitivity functions (SFs) of different variable-parameter combinations, relative sensitivity functions (RSFs) were used (Audenaert et al., 2010; Audenaert et al., 2011) rather than absolute SFs. The automated SF functionality in WEST was used and the steady-state RSF values were calculated using the parameter values indicated in Table 2. The RSF was calculated from the absolute sensitivity function (ASF) using the finite central difference method with a perturbation factor ξ of 5 x 10^{-2} (this perturbation factor was applicable for all variables of interest). This means that ASFs were calculated by (forward and backward) perturbing the default parameter value with an amount equal to the perturbation factor times the default value:

$$\frac{\partial y}{\partial \theta_j} = \frac{y(t,\theta_j + \zeta\theta_j) - y(t,\theta_j - \zeta\theta_j)}{2\zeta\theta_j} \quad (1)$$

in which y(t, θ_j) represents the output variable, θ_j represents the nominal parameter value and ξ is the perturbation factor.

RSFs are then calculated as follows:

$$RSF = \frac{ASF \times \theta}{y(t,\theta)} \quad (2)$$

A RSF less than 0.25 indicates that the parameter is not influential. Parameters are moderately influential when 0.25<RSF<1. When 1<RSF<2 and RSF>2, the parameter seems to be very and extremely influential, respectively (Audenaert et al., 2010). The sign of the RSF value specifies if raising the parameter impacts the variable in a positive (higher variable value) or negative (lower variable value) way. It should be noted that a local SA is a one-factor-at-a-time method which implies that only one parameter is perturbed at a time while all others are kept at their nominal value (Saltelli et al., 2005).

The sensitivity of the ozone and $HO^{\bullet}$ concentrations to all model parameters was investigated. Since these concentrations never reach steady state in the semi-batch reactor, the sensitivity functions also do not reach stable values. For this reason, the maximum RSF value was used in the graphical presentation of the results. For the flow-through reactor, the steady-state RSF values were used.

2.4. Global sensitivity analysis

2.4.1. Background

In contrast to a local sensitivity analysis, a global SA is performed by varying all parameters at the same time and over a broader range. Consequently, the results of global SAs are multidimensional averages: the impact of a parameter variation on the process is assessed, while all other parameters are also varying (Neumann et al., 2009; Saltelli et al., 2005). Prior to a global SA, two important properties are assigned to each parameter of interest: a range in which the parameter may vary and a probability density function (PDF) of the parameter in that range. Subsequently, by means of Monte Carlo simulation, a high number of independent samples are drawn from the parameter space, thereby accounting for the predefined parameter properties. Each sample represents a certain set of parameter values for which a separate simulation is run.

Global sensitivities in this study were calculated by means of linear regression (Saltelli et al., 2005). A linear model that describes the relation between a certain variable y (e.g. aqueous ozone concentration) and a number of n studied parameters (θ_i) is derived from the output of the Monte Carlo simulation. The linear model $y(\theta_1, \theta_2,\ldots, \theta_n)$ contains the parameter values with their respective regression coefficients. The regression coefficients are a measurement for the linear dependency between the output variable and the respective parameters. After a standardization of the regression coefficients (Saltelli et al., 2005), the t-statistic value of the standardized regression coefficients (SRCs) is calculated from the standard errors of the regression coefficients. The larger this tSRC value, the more influence a certain parameter has on the model output. If the t-statistic value is larger than 1.96, then the parameter significantly impacts the variable at the 5% confidence level.

A detailed description of performing global SAs and the statistical calculation can be found elsewhere (Saltelli et al., 2005).

2.4.2. Practical application

Parameters that were found to be important during the local SA were adopted in the global SA. An additional parameter related to $HO^{\bullet}$ scavenging by bicarbonate (k_{17}) was also considered. An interval was assigned to each of them, based on literature or laboratory experience. A uniform PDF was chosen which is characterized by a lower and upper bound. The parameters with their respective sampling intervals are given in Table 4. Latin Hypercube Sampling (LHS) was used as a sampling method to provide input for the Monte Carlo simulation. This is a commonly used and effective sampling technique (Saltelli et al., 2005). In total, 900 simulations were run (i.e. 100 simulations per parameter). The flow-through reactor was used to perform the global SA. To study the effect of scavenger levels on output sensitivity and uncertainty, a dynamic influent with changing C_T and [DOM] was used. The influent was characterized by four regions: (i) low C_T and low [DOM] (4000-5000s), (ii) high C_T and low [DOM] (5000-6000s), (iii) high C_T and high [DOM] (6000-7000s) and (iv) low C_T and high [DOM] (7000-8000s). The influent composition was tentatively chosen and is depicted in Figure 1 as function of time. Flow rate and all other concentrations were kept fixed. The first 4000s, the influent composition was kept constant in order to allow the reactor to reach steady state.

Table 4: Model parameters and confidence intervals used in the global SA

	Lowerbound	**Upperbound**		**Source of uncertainty interval**
k_1	40	100	$M^{-1}s^{-1}$	(Bezbarua and Reckhow, 2004; Fabian, 2006)
k_2	2.2×10^6	5.5×10^6	$M^{-1}s^{-1}$	(Bezbarua and Reckhow, 2004; Fabian, 2006)
k_9	1×10^8	3×10^9	$M^{-1}s^{-1}$	(Fabian, 2006)
k_{11}	0.045	0.125	$M^{-1}s^{-1}$	(Bezbarua and Reckhow, 2004; Lovato et al., 2009)
k_{12}	2×10^{10}	5×10^{10}	$M^{-1}s^{-1}$	(Bezbarua and Reckhow, 2004; Westerhoff et al., 1997)
k_{17}	8×10^6	9×10^6	$M^{-1}s^{-1}$	(Westerhoff et al., 1997)
k_{28}	1×10^8	1×10^9	$M^{-1}s^{-1}$	(Westerhoff et al., 1997)
$[O_3^*]$	5.4×10^5	6.6×10^5	M	Laboratory experience
k_La	1.35×10^3	1.65×10^3	s^{-1}	Laboratory experience

Besides as an input for the global SA, the data of the Monte Carlo simulation was used to perform uncertainty analysis on ozone and $HO^{\bullet}$ concentrations. The 50^{th}, 95^{th} and 5^{th} percentiles as function of time of these species were calculated.

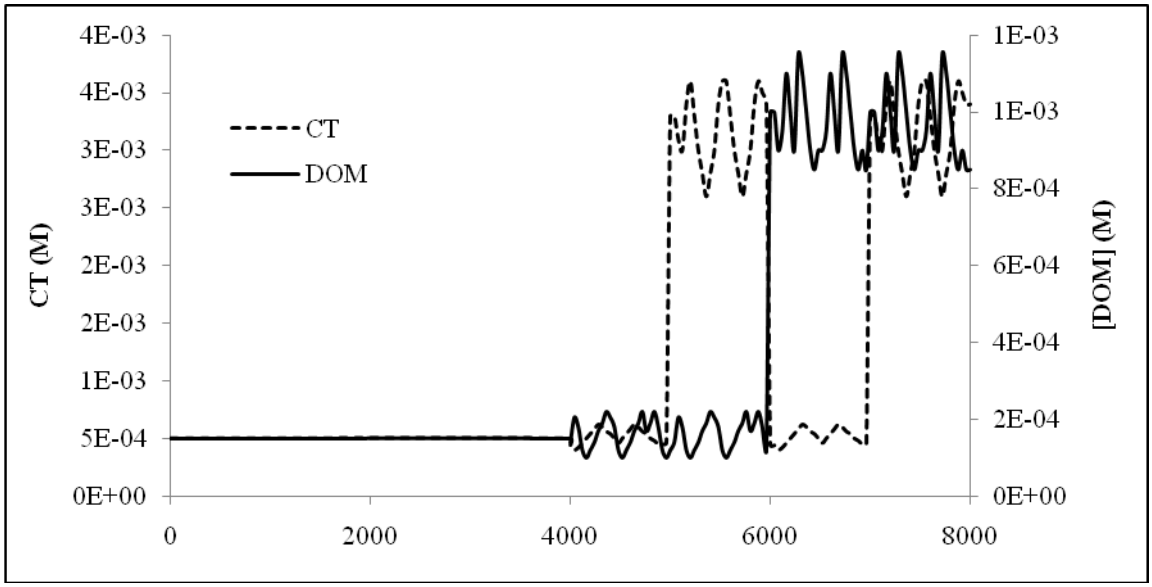

Figure 1: C_T and [DOM] levels of the dynamic influent used in the global SA as function of time

3. RESULTS AND DISCUSSION

3.1. Local sensitivity analysis

Results of local SAs for the semi-batch and flow-through reactor are presented in Figure 2 and Figure 3, respectively. The local SAs were performed at different concentrations of $HO^{\bullet}$ scavenging species (DOM and inorganic carbon). The parameters presented are the only parameters that were found to impact the ozone or $HO^{\bullet}$ concentration. Consequently, parameters involving reactions with inorganic carbon (characterized by rate constants k_{13}-k_{26}) have no impact on the process. Furthermore, it can be noticed that the sensitivity of the aqueous ozone concentration to parameter k_1 (related to the initiation reaction) is gradually decreasing with higher levels of scavengers. This finding is even more illustrated in Figure 4, where the sensitivity of the ozone concentration to k_1 is presented as function of the scavenger concentration. At very low scavenger levels, radical-induced ozone decay is of major importance. An increase of the chain initiation will almost directly lead to a higher ozone consumption as the major fate of the chain carriers is reaction with ozone. Higher scavenger levels will lead to a shift of the fate of $HO^{\bullet}$ to reaction with DOM (or inorganic carbon). This shift is clearly illustrated by the decreasing importance of k_9 and increasing importance of k_{28} with an increasing scavenging rate (see Table 1 for reaction numbers). The positive influence of k_1 on the $HO^{\bullet}$ concentration, however, is independent of the scavenger concentration (Figures 2 and 3). The effect of inorganic carbon only becomes clear when very low DOM concentrations are present and provided C_T is sufficiently high (Figure 4). Figures 2 and 3 also show that k_2 and the protonation constant of the hydroperoxyl ion (k_{12}) significantly impact the process at low scavenger concentrations. Again, this can be explained by the increased importance of the radical chain at low levels of scavengers. The second initiation step (reaction between ozone and the hydroperoxyl ion) is an important rate determining step. The protonation constant of the hydroperoxyl ion is four orders of magnitude higher than k_2

and hence, production of hydrogen peroxide will significantly slow down the chain initiation. It is already recognized that the addition of hydrogen peroxide to enhance chain initiation is only of value at high ozone and/or hydrogen peroxide concentrations, due to the slow dissociation and initiation reactions (Buffle et al., 2006a).

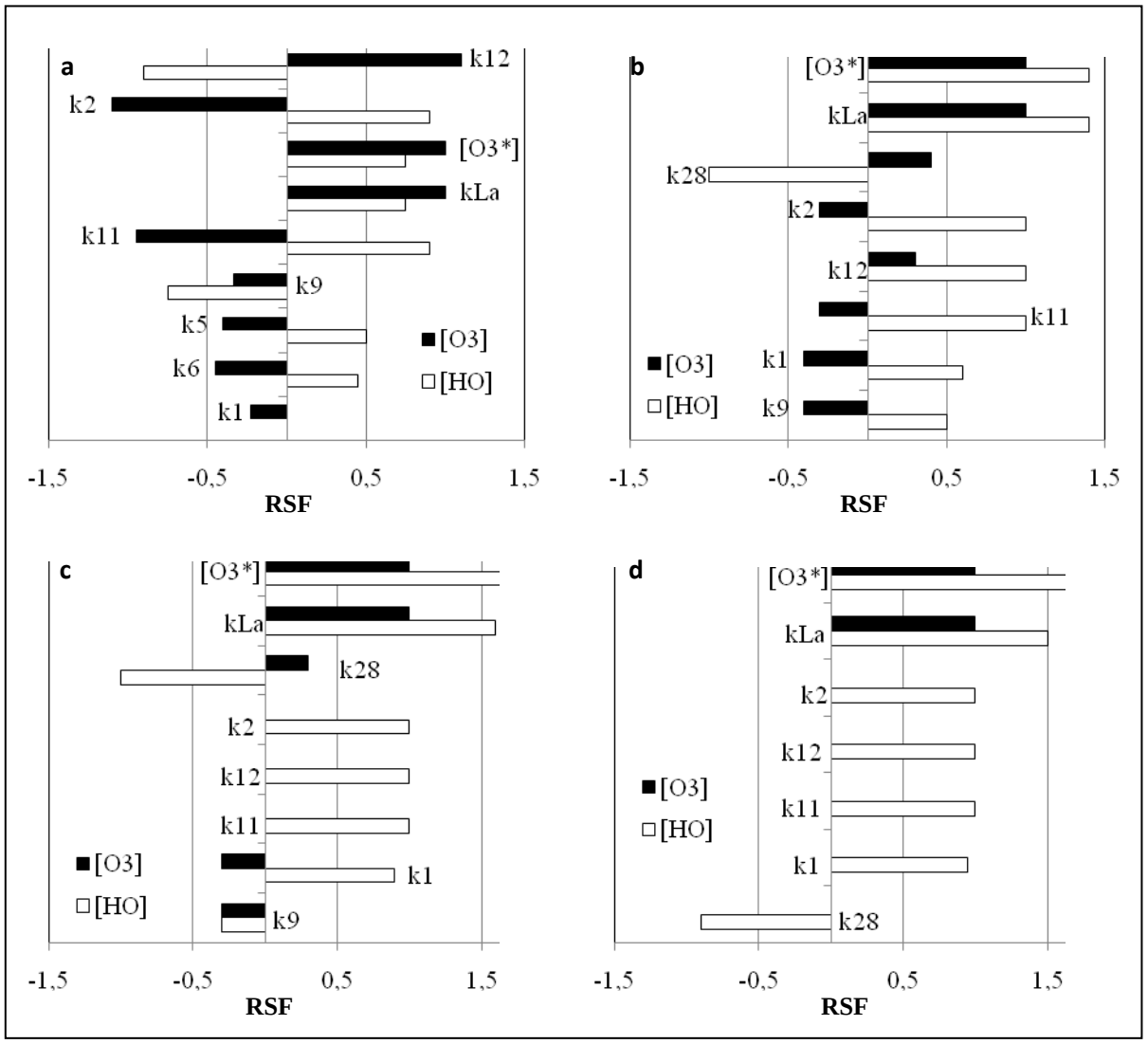

Figure 2: Results of local SA; sensitivity of O_3 and $HO^{\bullet}$ concentrations to most influential parameters in a semi-batch reactor (Tornado plot). Parameters sorted from most to least influential. (a) $[DOM]_0$= 0 mM and $[HCO_3^-]_0$= 0 mM, (b) $[DOM]_0$= 0.2 x10^{-3} mM;[$C_T]_0$= 0.2 x10^{-3} mM, (c) $[DOM]_0$= 16.7 x10^{-3} mM and $[C_T]_0$= 10 x10^{-3} mM, (d) $[DOM]_0$= 1 mM and $[C_T]_0$= 3.3 mM

The mass-transfer related parameters k_La and $[O_3*]$ are of major importance in all cases (RSF≥1), with the latter being the most influential parameter. Hence, it is of extreme importance that these parameters are determined with high accuracy. However, these parameters are highly dependent on many physical and chemical parameters (Beltrán, 2004; Kumar and Bose, 2004). Consequently, estimating these parameters at a high level of confidence will not be easily accomplished, especially at full-scale. Kumar and Bose (2004)

in their study concluded that discrepancies between experimental and modeled ozone concentrations were almost totally due to uncertainties in k_La and $[O_3^*]$ and not due to effects related to the mechanistic model under study.

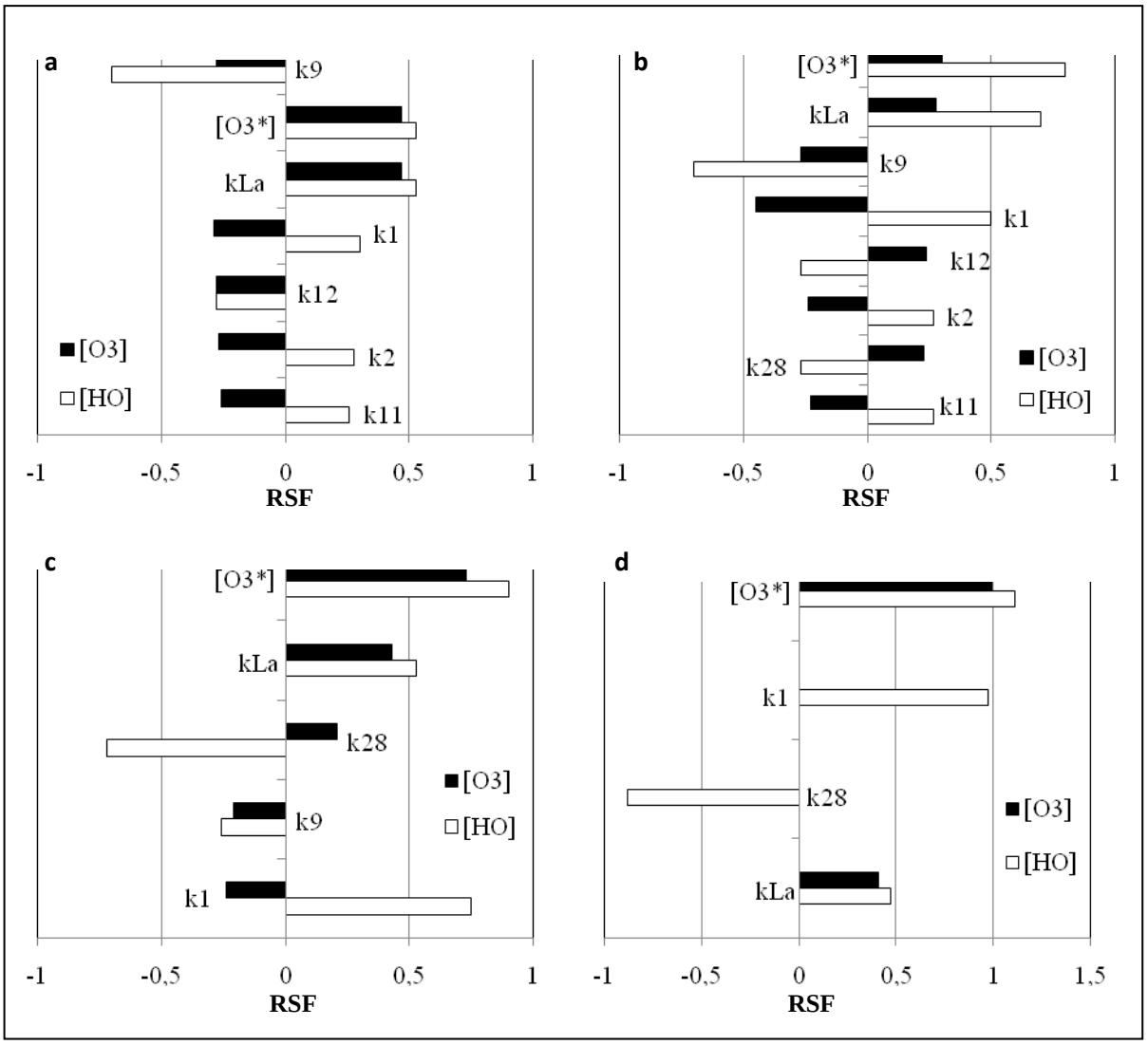

Figure 3: Results of local SA; sensitivity of O_3 and $HO^{\bullet}$ concentrations to most influential parameters in a flow-through reactor (Tornado plot). Parameters sorted from most to least influential. (a) $[DOM]_0$= 0 mM and $[C_T]_0$= 0 mM, (b) $[DOM]_0$= 0.2 x10^{-3} mM;[$C_T]_0$= 0.2 x10^{-3} mM, (c) $[DOM]_0$= 16.7 x10^{-3} mM and $[C_T]_0$= 10 x10^{-3} mM, (d) $[DOM]_0$= 1 mM and $[C_T]_0$= 3.3 mM

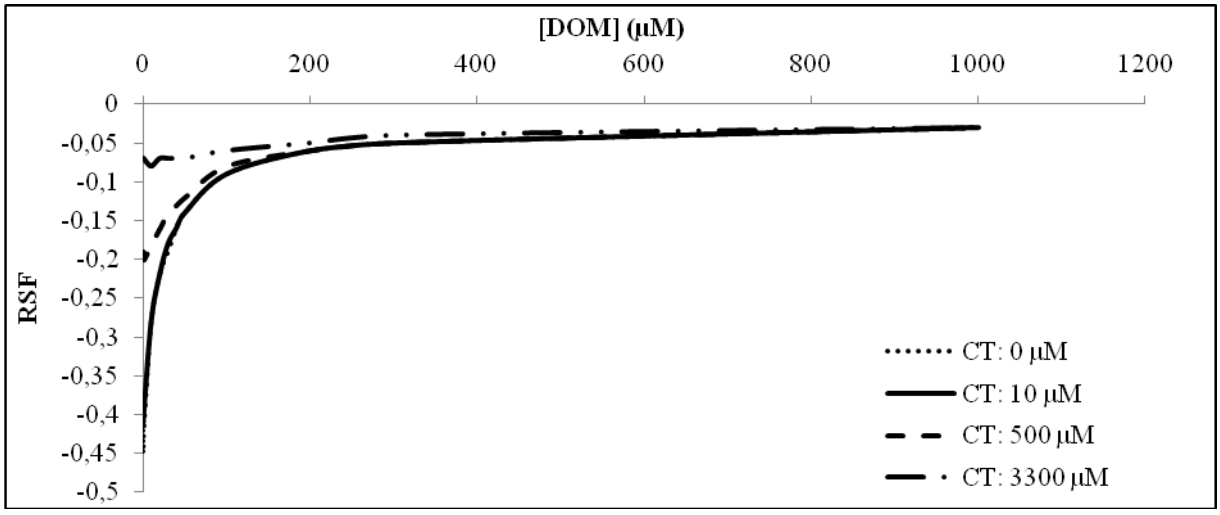

Figure 4: Sensitivity of $[O_3]$ to parameter k_1 as function of [DOM] and $[C_T]$ in a flow-through reactor

At low DOM concentrations, the ozone concentration in a semi-batch reactor showed a dynamic behaviour which can be clearly derived from the RSF as shown in Figure 5. During a first phase, sufficient DOM was present to scavenge all hydroxyl radicals which allowed the aqueous ozone concentration to increase. The rate constant describing scavenging by DOM (k_{28}) positively influenced the ozone concentration (the grey dashed line (CRS=0) was added for clarification). When DOM becomes limiting, however, more hydroxyl radicals are available for direct ozone decomposition. In this second phase, the rate constant became negatively influential as rising this parameter implied NOM to be depleted faster and hence, less radicals can be scavenged leading to lower ozone concentrations. As of the moment where all DOM was depleted, the sensitivity function reached its maximum value (RSF=-5.8). Consequently, at very low DOM concentrations, the ozone concentration shows to be extremely sensitive to k_{28} (|RSF|>2). In a third phase, the ozone concentration significantly decreased and the sensitivity function almost reached zero.

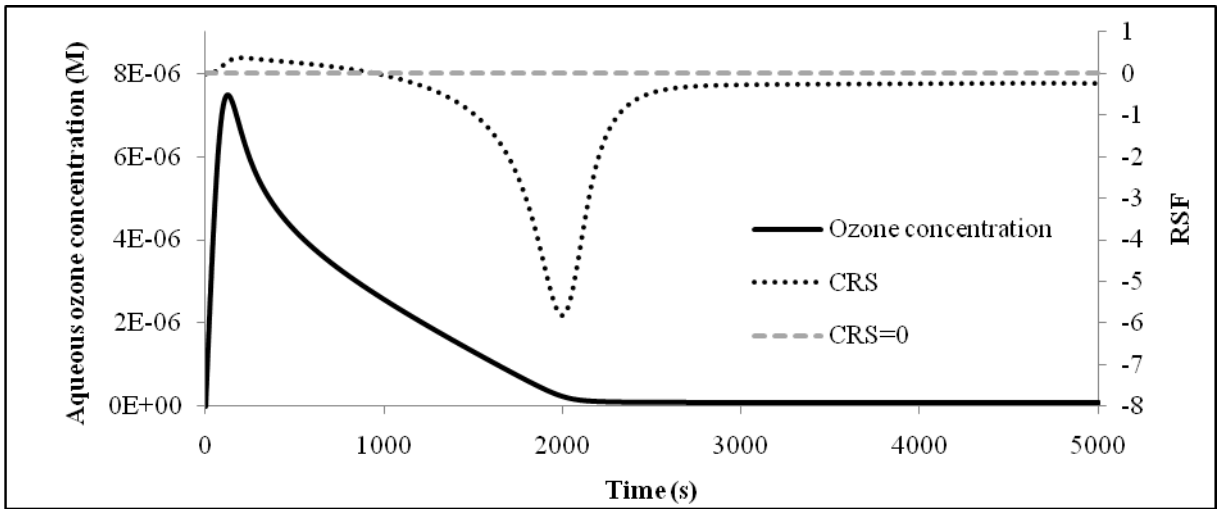

Figure 5: Sensitivity function of k_{28} with respect to the aqueous ozone concentration; $[NOM]_0$=0.1 µM

The extreme importance of DOM at very low concentrations has some important practical implications. Westerhoff et al. (1997) studied the SHB model using a batch reactor. Despite the fact that Milli-Q (ultrapure) water was used, the authors considered the presence of residual organic impurities with a concentration of 0.2 mg C L^{-1} (16.7 µM) (Westerhoff et al., 1997). The reaction sequence was therefore extended with a simple $HO^{\bullet}$ scavenging reaction with a second order rate constant of 2 x 10^8 $M^{-1}s^{-1}$. A satisfactory model prediction of the ozone decomposition profile could be obtained. Lovato et al. (2009) used the SHB model to describe ozone decomposition in a 11.5 L batch reactor at pH 4.8. The authors showed that the SHB model in its original form severely overestimated the ozone decay (Lovato et al., 2009). In order to obtain better fits, the model was modified. The reactor filled with ultrapure water was, however, assumed to be totally free of residual impurities and in contrast to the study of Westerhoff et al. (1997), the model did not account for these inhibiting substances. Figure 6 shows the measured ozone data adopted from Lovato et al. (2009). The solid line represents a simulation in which the water was considered to be free of impurities (analogous to Lovato et al. (2009)). The dashed line is representing a simulation in which very low concentrations of impurities (tentatively chosen) were considered ($[DOM]_0$=0.1 µM, C_T=10 µM). It can be clearly observed from this figure that extremely low levels of impurities have a significant impact on model predictions. Consequently, impurities should always be considered in ultrapure water systems.

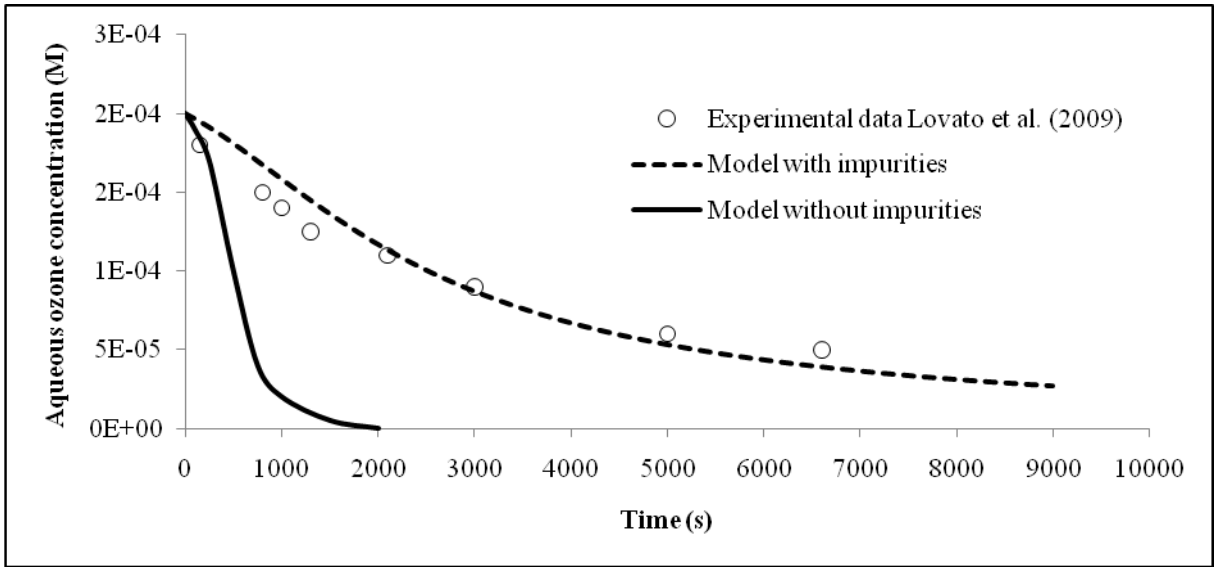

Figure 6: The effect of low levels of impurities on the modelled ozone concentration; experimental data points were adopted from Lovato et al. (2009)

3.2. Global sensitivity analysis

Results of the global SA for the ozone and $HO^{\bullet}$ concentration are presented in Figure 7. The tornado plots are comparable to those of the local SA conducted in the presence of scavengers (Figure 3). Therefore, only the most remarkable differences will be discussed in this section.

Compared to the results of local SAs, the sensitivity of the predicted ozone concentration to parameters [O_3*] and k_La is even more pronounced and very significant (tSRC>1.96). Contrarily, the impact of these parameters on the $HO^{\bullet}$ concentration is less visible but still significant. Rate constant k_1 is again classified as an influential parameter with respect to both the ozone and $HO^{\bullet}$ concentration. Parameter k_{28} is the far most influential parameter with regard to the $HO^{\bullet}$ concentration. The importance of this parameter was also noticeable during local SAs, but to a lower extent. Probably the large interval that was defined for this parameter (Table 4) is the underlying reason for this observation. The parameter was allowed to uniformly vary over one order of magnitude. In other words, there are places in the parameter space where the parameter becomes more important compared to the region studied in the local SA. This demonstrated the added value of a global SA. As expected, $HO^{\bullet}$ scavenging by bicarbonate was not found to significantly impact the output. Parameter k_{17} is of minor importance in both cases. Also rate constant k_9 seemed to be less important, at least with respect to the $HO^{\bullet}$ concentration. Results of local SAs revealed that this parameter is only influential at (very) low scavenger concentrations.

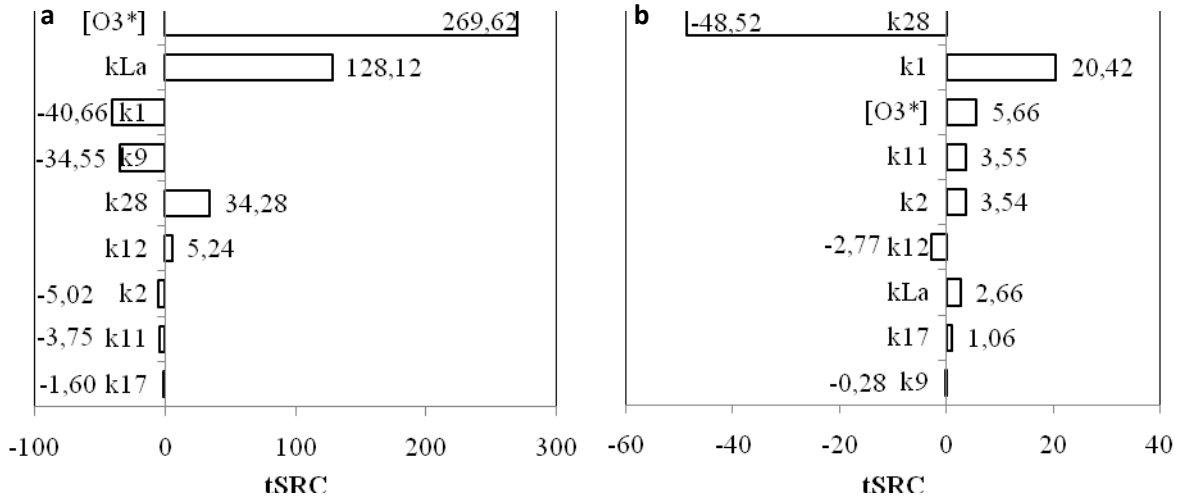

Figure 7: Results of global SA; sensitivity of O_3 (a) and $HO^{\bullet}$ concentrations (b) to most influential parameters in a flow-through reactor (Tornado plot). Parameters sorted from most to least influential.

3.3. Uncertainty analysis of output

The 50^{th} percentile of ozone and $HO^{\bullet}$ concentrations and their respective 95% confidence intervals as function of time are presented in Figure 8 and Figure 9, respectively. Aqueous ozone and $HO^{\bullet}$ radical concentrations are clearly building up due to gas-liquid mass transfer. Fluctuations in the average concentrations are caused by dynamics in the influent. From Figure 8, the different phases (varying scavenger concentrations) can be hardly distinguished suggesting that scavenger levels have a low impact on the ozone concentration profile. SAs revealed that especially at low concentrations (µM range) of DOM and inorganic carbon, ozone is susceptible to changes in the $HO^{\bullet}$ scavenging rate. DOM and C_T levels of the dynamic influent were in the mM range, explaining a relative stable ozone concentration profile and confidence interval. In contrast, the $HO^{\bullet}$ concentration profile clearly reflects the

different phases. Uncertainty significantly decreases from 5000s as more inorganic carbon is entering the reactor. The average $HO^{\bullet}$ concentration, however, only significantly decreases when the DOM level is increased (6000s). From this moment, a drastic reduction of the uncertainty interval occurs.

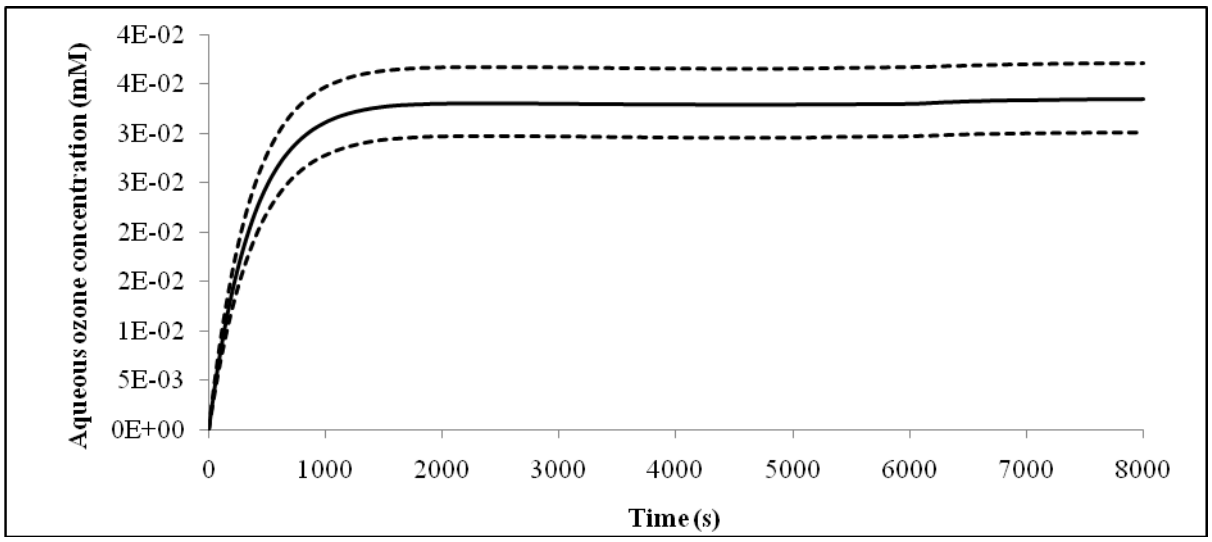

Figure 8: 50th percentile of predicted ozone concentration (solid line) with 95% confidence interval (dashed lines) as function of time; plot derived from 900 Monte Carlo runs

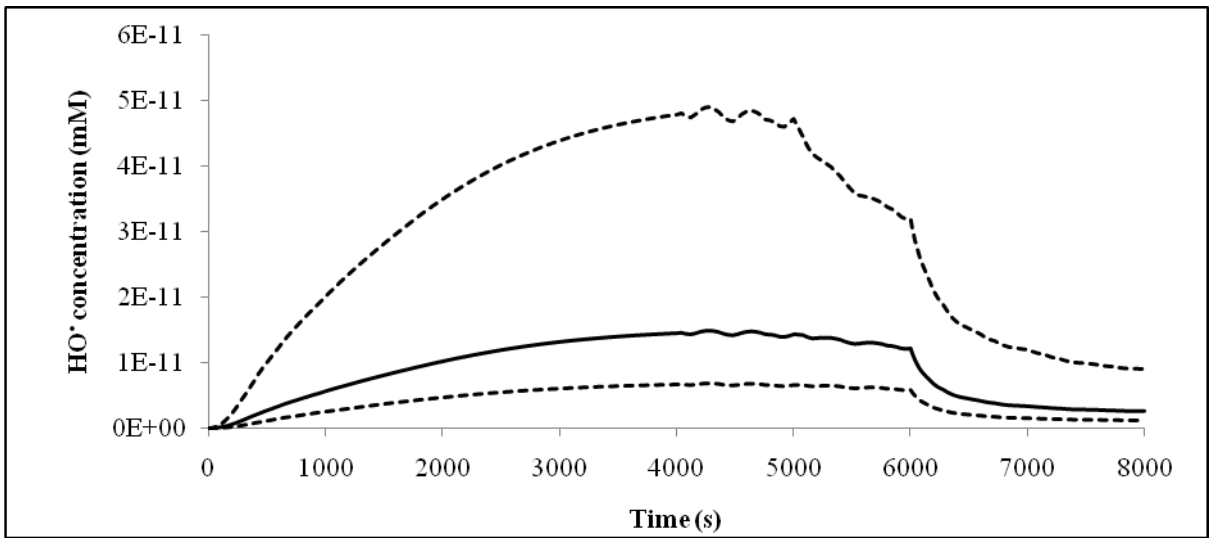

Figure 9: 50th percentile of predicted $HO^{\bullet}$ concentration (solid line) with 95% confidence interval (dashed lines) as function of time; plot derived from 900 Monte Carlo runs

Based on the global SA, most of the uncertainty in $HO^{\bullet}$ concentration is caused by a not well defined rate constant describing scavenging by DOM (k_{28}). This illustrates the importance of including more detailed DOM reaction sequences in future models in order to reduce this uncertainty. A reliable estimation of $HO^{\bullet}$ exposure is of vital importance for DOM moieties that slowly react with ozone and hence, are primarly removed by $HO^{\bullet}$ induced oxidation (Neumann et al., 2009; Zimmermann et al., 2011).

4. CONCLUSIONS

In this study, the extensive SBH model consisting of a set of elementary reactions describing aqueous ozone decomposition was investigated in detail by means of sensitivity analysis. The model was extended with a simple equation describing hydroxyl radical scavenging by DOM to study the effect of varying scavenger concentrations. Local SAs revealed that only seven of the twenty-eight first and second order rate constants showed to impact ozone and $HO^{\bullet}$ concentrations. Processes involving $HO^{\bullet}$ scavenging by inorganic carbon were of minor importance. The effect of inorganic carbon only became clear when very low DOM concentrations were present and provided C_T was sufficiently high. Mass-transfer related parameters k_La and $[O_3^*]$ were of major importance in all cases. Hence, it is of extreme importance that these parameters are determined with high accuracy, which is a rather difficult task given the many physical and chemical parameters affecting them. It was shown that the aqueous ozone concentration is extremely sensitive to parameters involving DOM at very low scavenger concentrations. Hence, impurities should always be considered in models, even in ultrapure water systems.

Results of a global SA were to a high extent comparable to these of local SAs. The importance of the mass-transfer related parameters was even more pronounced. Furthermore, the global SA revealed that a detailed description of reactions involving DOM is of vital importance as their related parameters seem to be very important. Uncertainty analysis showed that especially the $HO^{\bullet}$ concentration is susceptible to variations in influent composition. The uncertainty regarding this species significantly reduced with increasing levels of scavengers and especially DOM.

It was shown in this study that simplification of the elementary radical scheme should be considered. For example, it is questionable if inorganic reactions should be included when DOM levels are sufficiently high. Additionally, some dissociation reactions might be discarded if the model is used within a predefined pH range. On the other hand, a model extension with regard to reactions involving DOM should be considered in order to improve the applicability of future wastewater ozonation models. It should, however, be highlighted that in this study DOM was only considered as inhibitor. Direct reactions with ozone, promoting and initiating properties of DOM were not included. Hence, this study is a detailed analysis of the SHB model, but did not include all important reaction steps of DOM. This will be an important issue in future research.

5. ACKNOLEDGEMENTS

This research was partially funded by a University College West Flanders PhD research grant and is in close cooperation with the Veg-i-Trade FP7-KBBE-2009-3 project.

6. REFERENCES

Audenaert, W. T. M., Callewaert, M., Nopens, I., Cromphout, J., Vanhoucke, R., Dumoulin, A., Dejans, P., and Van Hulle, S. W. H. (2010). Full-scale modelling of an ozone reactor for drinking water treatment. *Chemical Engineering Journal* **157**, 551-557.

Audenaert, W. T. M., Vermeersch, Y., Van Hulle, S. W. H., Dejans, P., Dumoulin, A., and Nopens, I. (2011). Application of a mechanistic UV/hydrogen peroxide model at full-scale: Sensitivity analysis, calibration and performance evaluation. *Chemical Engineering Journal* **171**, 113-126.

Beltrán, F. J. (2004). "Ozone Reaction Kinetics for Water and Wastewater Systems," CRC Press, Florida, USA.

Bezbarua, B. K., and Reckhow, D. A. (2004). Modification of the standard neutral ozone decomposition model. *Ozone-Science & Engineering* **26**, 345-357.

Buffle, M. O., Schumacher, J., Meylan, S., Jekel, M., and von Gunten, U. (2006a). Ozonation and advanced oxidation of wastewater: Effect of O-3 dose, pH, DOM and HO center dot-scavengers on ozone decomposition and HO center dot generation. *Ozone-Science & Engineering* **28**, 247-259.

Buffle, M. O., Schumacher, J., Salhi, E., Jekel, M., and von Gunten, U. (2006b). Measurement of the initial phase of ozone decomposition in water and wastewater by means of a continuous quench-flow system: Application to disinfection and pharmaceutical oxidation. *Water Research* **40**, 1884-1894.

Buhler, R. E., Staehelin, J., and Hoigne, J. (1984). OZONE DECOMPOSITION IN WATER STUDIED BY PULSE-RADIOLYSIS .1. HO2/O2-AND HO3/O3- AS INTERMEDIATES. *Journal of Physical Chemistry* **88**, 2560-2564.

Elovitz, M. S., and von Gunten, U. (1999). Hydroxyl radical ozone ratios during ozonation processes. I-The R-ct concept. *Ozone-Science & Engineering* **21**, 239-260.

Fabian, I. (2006). Reactive intermediates in aqueous ozone decomposition: A mechanistic approach. *Pure and Applied Chemistry* **78**, 1559-1570.

Henze, M., Gujer, W., Mino, T., and van Loodsrecht, M. (2000). "Activated sludge models ASM1, ASM2, ASM2d and ASM3," IWA Publishing, London.

Hindmarsh, A. C., and Petzold, L. R. (1995). Algorithms and software for ordinary differential equations and differential-algebraic equations. *Computers in Physics* **9**, 148-155.

Kumar, R., and Bose, P. (2004). Development and experimental validation of the model of a continuous-flow countercurrent ozone contactor. *Industrial & Engineering Chemistry Research* **43**, 1418-1429.

Lovato, M. E., Martin, C. A., and Cassano, A. E. (2009). A reaction kinetic model for ozone decomposition in aqueous media valid for neutral and acidic pH. *Chemical Engineering Journal* **146**, 486-497.

Lovato, M. E., Martín, C. A., and Cassano, A. E. (2011). A reaction–reactor model for O_3 and UVC radiation degradation of dichloroacetic acid: The kinetics of three parallel reactions. *Chemical Engineering Journal* **171**, 474-489.

Neumann, M. B., Gujer, W., and von Gunten, U. (2009). Global sensitivity analysis for model-based prediction of oxidative micropollutant transformation during drinking water treatment. *Water Research* **43**, 997-1004.

Saltelli, A., Ratto, M., Tarantola, S., and Campolongo, F. (2005). Sensitivity analysis for chemical models. *Chemical Reviews* **105**, 2811-2827.

Staehelin, J., Buhler, R. E., and Hoigne, J. (1984). OZONE DECOMPOSITION IN WATER STUDIED BY PULSE-RADIOLYSIS .2. OH AND HO4 AS CHAIN INTERMEDIATES. *Journal of Physical Chemistry* **88**, 5999-6004.

Van Geluwe, S., Braeken, L., and Van der Bruggen, B. (2011). Ozone oxidation for the alleviation of membrane fouling by natural organic matter: A review. *Water Research* **45**, 3551-3570.

Vanhooren, H., De Pauw, D., and Vanrolleghem, P. A. (2003). Induction of denitrification in a pilot-scale trickling filter by adding nitrate at high loading rate. *Water Science and Technology* **47**, 61-68.

Westerhoff, P., Aiken, G., Amy, G., and Debroux, J. (1999). Relationships between the structure of natural organic matter and its reactivity towards molecular ozone and hydroxyl radicals. *Water Research* **33**, 2265-2276.

Westerhoff, P., Mezyk, S. P., Cooper, W. J., and Minakata, D. (2007). Electron pulse radiolysis determination of hydroxyl radical rate constants with Suwannee river fulvic acid and other dissolved organic matter isolates. *Environmental Science & Technology* **41**, 4640-4646.

Westerhoff, P., Song, R., Amy, G., and Minear, R. (1997). Applications of ozone decomposition models. *Ozone-Science & Engineering* **19**, 55-73.

Zimmermann, S. G., Wittenwiler, M., Hollender, J., Krauss, M., Ort, C., Siegrist, H., and von Gunten, U. (2011). Kinetic assessment and modeling of an ozonation step for full-scale municipal wastewater treatment: Micropollutant oxidation, by-product formation and disinfection. *Water Research* **45**, 605-617.

APPENDIX

Composing mass balances from the Gujer matrix

As an example, the mass balance of ozone is derived from the Gujer matrix. The mass balance is built up by first multiplying each matrix element of the column of O_3 by the reaction rate at the same row of the element. A summation of these products yields the conversion terms of the mass balance:

$$r_{O_3} =$$
$$-k_1 \times [O_3] \times [OH^-] - k_2 \times [O_3] \times [HO_2^-] - k_5 \times [O_3] \times [O_2^{-\bullet}] - k_9 \times [O_3] \times [OH^\bullet]$$
$$+k_{23} \times [CO_3^{-\bullet}] \times [HO_2^-] + k_L a \times ([O_3^*] - [O_3])$$

To describe the bicarbonate concentration in a single completely stirred tank reactor (CSTR) operating in a continuous flow mode, transportation terms must be added as follows:

$$r_{O_3} = \frac{Q}{V}([O_3]_{in} - [O_3]_{out})$$
$$-k_1 \times [O_3] \times [OH^-] - k_2 \times [O_3] \times [HO_2^-] - k_5 \times [O_3] \times [O_2^{-\bullet}] - k_9 \times [O_3] \times [OH^\bullet]$$
$$+k_{23} \times [CO_3^{-\bullet}] \times [HO_2^-] + k_L a \times ([O_3^*] - [O_3])$$

Where Q represents the flow rate (L s^{-1}) and V is representing the volume of the tank (L).